High Speed Target Pursuit and Asymptotic Stability in Mobile Robotics

Martin D. Adams, *Associate Member, IEEE*

***Abstract*—Many mobile robot path planning algorithms, produce changing intermediate goal coordinates for a mobile robot to pursue, and provide motoring speed/torque signals based upon local sensor information and the position of the global target. This is often done with little or no regard for the low level vehicle dynamics, which, in practice, must be taken into account for efficient path planning. Therefore, in this article mobile robot path planning parameters are related to the application of a correct, general control law. It will be shown that nonlinear control analysis provides a useful tool for quantifying various path planning parameters in order that stable asymptotic convergence of a mobile robot to its target is guaranteed. Contrary to previous work, this analysis allows a deceleration zone to be quantified which surrounds any mobile robot's goal. Results show that near time optimal goal seeking is possible with real vehicles having simple proportional or integral controllers only.**

***Index Terms*—Asymptotic stability, dual input describing function, limit cycle, Lyapunov function, mobile robot, nonlinear control, potential field.**

I. Introduction

In the past, "low level" control and so called "high level" path planning have often been separated in an attempt to remove the burden of a mobile vehicle's motor control theory from the researcher. The philosophy presented here is that efficient mobile robot trajectory execution, can only result from a path planning algorithm which takes into account the "lower level" motor dynamics of the vehicle concerned, a philosophy which has been adopted by few researchers in the past [1]–[4]. Therefore in this article, mobile robot path planning parameters are related to the application of a correct control law. Inspiration is taken from the work by Daniel E. Koditschek [5], as a control law for a mobile vehicle is derived from considerations of its total energy, when it moves under the influence of an artificial potential field.

Any real mobile vehicle under the influence of a potential field navigation technique, automatically inherits a nonlinear control system which can be analyzed for stability and convergence using Lyapunov functions.

The *dual input describing function* method is used to determine the general equations necessary to form a relationship between the potential field algorithm parameters, and the distance of any mobile robot from its target at which a *stable oscillation* can occur. The derived theory is used to reach a target as fast as possible and guarantee that no limit cycle can occur. It will be demonstrated that internal PID speed/torque control, under a potential field navigation algorithm, does not allow faster convergence of a mobile robot to its goal than simple proportional or integral control only. The theoretical analysis is applied to two mobile vehicles.

Manuscript received May 13, 1997; revised December 8, 1998. This paper was recommended for publication by Associate Editor J. Burdick and Editor V. Lumelsky upon evaluation of the reviewers' comments.

The author is with the European Semiconductor Equipment Centre (ESEC), Cham, Switzerland.

Publisher Item Identifier S 1042-296X(99)03387-X.

II. Relationship Between Navigation, Stability and Control

A. Control: Energy Considerations

The derivation of a relationship between navigation and control begins with the use of *artificial potential field* methods [5]–[10]. Consider an unknown potential function ψ which assigns a scalar value to every position within the plane surrounding a mobile robot observed by its sensor(s), and vanishes uniquely at the target with position vector $\mathbf{x}_d$, i.e., $\psi(\mathbf{x}_d) = 0$. The imaginary potential energy of the mobile robot is ψ and its kinetic energy T is given by

$$T = \frac{1}{2} M \dot{\mathbf{x}}^T \dot{\mathbf{x}} \tag{1}$$

where M represents the total mass of the mobile robot and $\dot{\mathbf{x}}$ its velocity vector within the plane. The total energy possessed by the robot is η given by

$$\eta = \frac{1}{2} M \dot{\mathbf{x}}^T \dot{\mathbf{x}} + \psi. \tag{2}$$

All nonconservative forces $\mathbf{F}_{\text{ext}}$ which act on the mobile robot are given by the Lagrange equation [11]

$$\frac{d}{dt}\left(\frac{\partial(T-\psi)}{\partial \dot{\mathbf{x}}}\right) - \frac{\partial(T-\psi)}{\partial \mathbf{x}} = \mathbf{F}_{\text{ext}} \tag{3}$$

which results in the expression

$$\mathbf{F}_{\text{ext}} = M\ddot{\mathbf{x}} + \nabla\psi. \tag{4}$$

Due to the linearity of the ∇ operator in (4), superposition can be used to form a single potential force function $\nabla\psi$ from discrete components. Hence, in general, the potential function is made up of two components, an attractive field ψ_{att}, and a repulsive field which is generated by the sensor data (see for example [12]) so that

$$\psi = \psi_{\text{att}} + \psi_{\text{rep}}. \tag{5}$$

The attractive field or "cost function" assigns scalar values, within the plane of action of the mobile robot, which vanish

uniquely at the target $\mathbf{x}_d$ and grow larger further away from $\mathbf{x}_d$. A linear control law results by using a quadratic Hooke's law function, as suggested by Volpe and Khosla [13][1]

$$\psi_{\text{att}} = \frac{1}{2}K_1(\mathbf{x}-\mathbf{x}_d)^T(\mathbf{x}-\mathbf{x}_d) \tag{6}$$

ψ_{rep} is to provide a field to control the influence of the environment upon the path of the vehicle, a detailed analyses of which can be found in [12] and [14].

From (5) and (6)

$$\nabla\psi = K_1(\mathbf{x}-\mathbf{x}_d) + \nabla\psi_{\text{rep}}. \tag{7}$$

From Lagrange's equation (3), $\mathbf{F}_{\text{ext}}$ in (4) is by definition dissipative. Therefore let

$$\mathbf{F}_{\text{ext}} = -K_2\dot{\mathbf{x}} \tag{8}$$

the negative sign indicating *dissipation*, $\dot{\mathbf{x}}$ the velocity vector of the mobile robot and K_2 a positive constant. Equation (4) can be used to derive a control law for a mobile vehicle. By substituting for $\nabla\psi$ [see (7)] and $\mathbf{F}_{\text{ext}}$ [see (8)] in the equilibrium force (4)

$$-K_2\dot{\mathbf{x}} = M\ddot{\mathbf{x}} + K_1(\mathbf{x}-\mathbf{x}_d) + \nabla\psi_{\text{rep}}. \tag{9}$$

By using the operator $s = \frac{\partial}{\partial t}$ and rearranging (9)

$$\dot{\mathbf{x}} = \frac{K_1}{K_2}\left[\mathbf{x}_d - \left(1 + s^2\frac{M}{K_1}\right)\mathbf{x} - \frac{1}{K_1}\nabla\psi_{\text{rep}}\right]. \tag{10}$$

Hence by considering the total energy of a mobile robot, when under the influence of an artificial potential field, a control law can be derived, namely that the desired velocity signal to the motors should be dependent upon both position and *acceleration* feedback of the robot. Equation (10) is a general control law since no assumptions have been made about the vehicle's dynamics, in terms of transferring $\dot{\mathbf{x}}$ into its position vector $\mathbf{x}$.[2]

Following the derivation of the control laws given in (10), the question: "Can the stability and hence convergence of the mobile robot to the desired position vector $\mathbf{x}_d$ be guaranteed?" must be answered.

B. Stability—Lyapunov's Direct Method

The use of Lyapunov functions can be useful for asymptotic stability analysis (see for example [16]). A candidate Lyapunov function $V(\mathbf{x},\dot{\mathbf{x}})$, for stability analysis, is the total energy of the mobile vehicle where, from (2), (5), and (6)

$$V(\mathbf{x},\dot{\mathbf{x}}) = \eta = \frac{1}{2}M\dot{\mathbf{x}}^T\dot{\mathbf{x}} + \frac{1}{2}K_1(\mathbf{x}-\mathbf{x}_d)^T(\mathbf{x}-\mathbf{x}_d) + \psi_{\text{rep}}. \tag{11}$$

Because $\mathbf{F}_{\text{ext}}$ represents a dissipative force in (8) the mobile robot's total energy must decrease for all non zero velocity states, as it pursues the target at $\mathbf{x}_d$. The dissipative force can be thought of, in mechanical terms, as an imaginary Rayleigh damper, [5]. It will now be shown, that the rate of increase of the mobile robot's energy is negative by using (2) and (4)

$$\frac{d\eta}{dt} = \frac{d\eta}{d\mathbf{x}}\frac{d\mathbf{x}}{dt} = (M\ddot{\mathbf{x}} + \nabla\psi)\dot{\mathbf{x}} = \mathbf{F}_{\text{ext}}\dot{\mathbf{x}} \tag{12}$$

which from (8) gives

$$\dot{V}(\mathbf{x},\dot{\mathbf{x}}) = \dot{\eta} = -K_2\dot{\mathbf{x}}^T\dot{\mathbf{x}}. \tag{13}$$

Hence if the total energy of the mobile robot is used as a Lyapunov function—i.e. $V(\mathbf{x},\dot{\mathbf{x}}) = \eta$ in the theorem stated above, the condition that the function is positive definite will be met only if the right hand side of (11) is always positive for all position and velocity states $\mathbf{x}$ and $\dot{\mathbf{x}}$ within the phase plane. Therefore

$$M\ddot{\mathbf{x}} + K_1(\mathbf{x}-\mathbf{x}_d) > -\nabla\psi_{\text{rep}}. \tag{14}$$

must be obeyed in order for $V(\mathbf{x},\dot{\mathbf{x}})$ to be positive definite. This inequality imposes an upper limit on the magnitude of $\nabla\psi_{\text{rep}}$. If the constraint is introduced that the velocity vector $\dot{\mathbf{x}}$ may never reach $\mathbf{0}$ until $\mathbf{x} = \mathbf{x}_d$, the desired position of the mobile robot, then $-\dot{\eta}$ [from (13)] will be positive definite also.

By using the speed controller given in (10) and shown in Fig. 1, the convergence of a mobile robot to a desired position $\mathbf{x}_d$ can be guaranteed, provided the following conditions are met.

Condition 1 *The local minimum of ψ is at $\mathbf{x} = \mathbf{x}_d$.* Upon receipt of a scan of the local environment, it must be arranged that the attractive force toward $\mathbf{x}_d$ plus the inertial force of the robot is *always* greater than the repulsive force, $\nabla\psi_{\text{rep}}$, generated from the sensor data [12], [14].

Condition 2 *Global Asymptotic Stability:* $\dot{\mathbf{x}}$ never reaches zero until $\mathbf{x} = \mathbf{x}_d$.

In order to navigate a vehicle safely, it intuitively seems that the repulsive force field, $\nabla\psi_{\text{rep}}$ would need the power to cancel or even reverse the overall force acting on it. In this case condition 1 would be violated. By allowing $\mathbf{F}_{\text{ext}}$ to reach zero or reverse, the well known problem of a *potential minimum* will be reached as the mobile robot's velocity state $\dot{\mathbf{x}}$ will reach zero before $\mathbf{x} = \mathbf{x}_d$, and its energy will no longer be decreasing.

The rest of this section discusses further the control aspects of the proposed system, since this forms the basis of the safe response of a real mobile vehicle to variable step inputs $\mathbf{x}_d$.

The velocity signal $\dot{\mathbf{x}}$ in Fig. 1 can assume any values, dictated by $\mathbf{x}_d$, $\mathbf{x}$ and $\nabla\psi_{\text{rep}}$. In reality of course, a real vehicle cannot travel at any speed and will be limited to $\pm\mathbf{U}$ m/s say. This is taken into account, in Fig. 1, by replacing the linear amplifier having gain K_1/K_2, with a nonlinear ideal saturation with the same gain but saturation levels of $\pm\mathbf{U}$. Examination of (11) and (13) will reveal that the total energy is still positive definite (the kinetic energy term is now simply bounded), and that the rate of increase of energy is still negative definite (but bounded between 0 and $-K_2\mathbf{U}^T\mathbf{U}$) under the same conditions 1 and 2.

[1] Note that Khosla and Volpe show that all other possible potential attraction laws reduce to quadratic attraction for small displacements anyway [13].

[2] Note that under a similar analysis, (9) can be rearranged to produce a desired *torque* signal, often used to drive motors [12], [15].

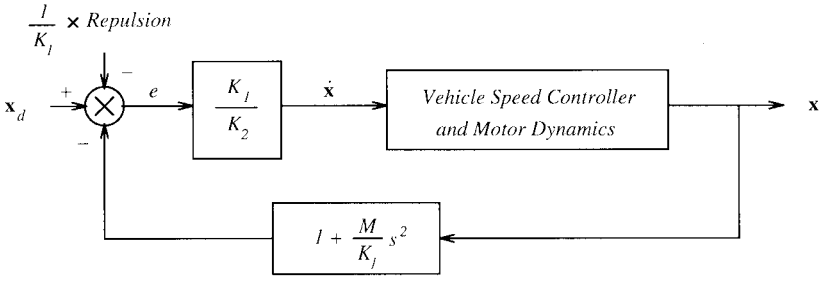

Fig. 1. Controller proposed by energy considerations of a mobile robot moving within an artificial potential field. The disturbance signal $\frac{1}{K_1} \times$ Repulsion represents the effect of the sensor data upon a vehicle's path.

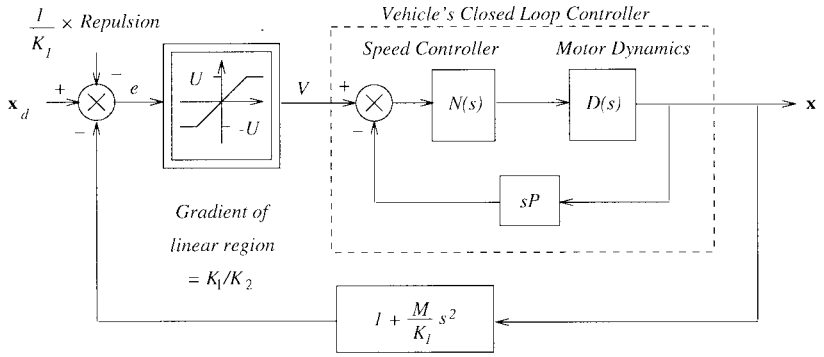

Fig. 2. Realistic control system for any vehicle with its own speed controller, under the influence of an artificial potential field.

The energy considerations have provided no insight into the possible numerical values of K_1 and K_2 (other than that they must both be positive) nor have they provided a method for relating the sensor data to the value of $\nabla\psi_{\text{rep}}$. A quantitative analysis of conditions 1 and 2 is necessary to provide the limiting values for K_1, K_2 and $\nabla\psi_{\text{rep}}$. The quantitative application of condition 1 involves the sensor data estimate $\nabla\psi_{\text{rep}}$, and is explained in [12].

It will be shown in Section III, that values for K_1 and K_2 depend upon the application of condition 2 under a nonlinear control system analysis.

III. Nonlinear Potential Attraction for a Mobile Vehicle

In previous literature, Khatib [8], Volpe and Khosla [13] and Warren [17] have suggested that, in practice, the influence of the linear potential attraction law surrounding a target should be limited so that a mobile robot can travel at maximum speed until this limiting region is reached. Once inside this region, the linear potential attractive force law should come into effect so that the mobile robot decelerates to a stand still at the target. The necessary size of this limiting region, beyond which the potential attraction saturates to a constant, has however, to our knowledge, never been quantified. The smaller this region is, the less time the mobile robot will take to reach its target [18]. It will be shown in this section that the application of condition 2 provides a quantitative analysis of the size necessary for this limiting region.

Under the more realistic restrictions of saturated speed inputs[3] to the motors driving a vehicle, Fig. 1 is transformed into Fig. 2. This figure shows the full control system derived so far, for any vehicle with its own *speed* controller $N(s)$ and motor dynamics $D(s)$. Particular transfer functions for $N(s)$ and $D(s)$ will be examined later in Section IV, but at present, the general effect of the saturation upon the speed signal V, input into a vehicle's speed controller, is considered.

To simplify the analysis of the complete control system in Fig. 2, the closed loop vehicle's speed controller and dynamics are replaced with their open loop equivalent $H(s)$—i.e.,

$$H(s) = \frac{N(s)D(s)}{1 + sPN(s)D(s)} \tag{15}$$

where P is the velocity feedback gain. $H(s)$ will be referred to later in this section.

In order not to obtain a limit cycle within the system, conditions must be imposed upon K_1 and K_2. If these conditions are violated, an oscillation with known amplitude and frequency will be observed as the vehicle performs oscillations about the equilibrium point, thus violating condition 2. The effect of the inertial term within the feedback loop of Fig. 2 will also be demonstrated. This term allows the gradient $\frac{K_1}{K_2}$ to be increased almost to the limiting condition of the nonlinearity becoming a perfect relay without observing oscillations, meaning that a mobile vehicle could theoretically approach its target at maximum speed until it is reached. This means that the nonlinearity could almost supply the motors with time optimal *bang bang* control. Limit cycle analysis is possible using Bendixson's theorem [19], multiple model approaches [20] or describing functions [21]. Since the system in Fig. 2 is split into a nonlinear amplifier driving linear motor dynamics, the describing function method is applied.

[3] or equivalently saturated torque inputs.

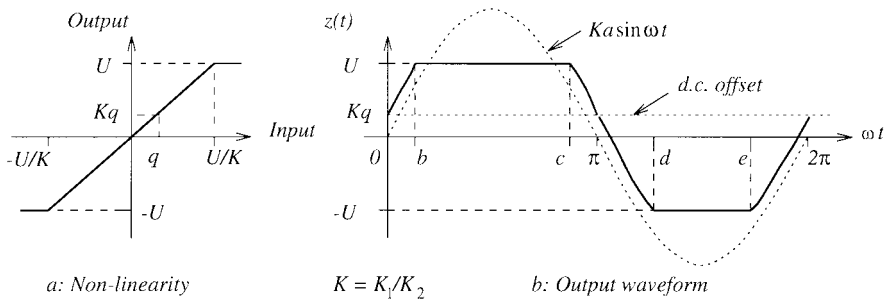

Fig. 3. Output waveform produced by the nonlinear saturation in response to the signal $w(t) = a\sin\omega t + q$ for $a > \frac{UK_2}{K_1} + q$. In the figure $K = K_1/K_2$.

A. Describing Function Analysis

Assume that there exists a stable limit cycle oscillation within the system. As the difference in the desired signal $\mathbf{x}_d$, the output $\mathbf{x}$ and any disturbance produced by the on board sensor approaches the steady state (i.e. the mobile moves toward convergence upon the target), there will be other signals superimposed onto the stable limit cycle oscillation. Assuming $H(s)$ has low pass frequency characteristics (as is the case with all motoring systems), the signals appearing at the input of the nonlinearity will be of the form

$$w(t) = a\sin\omega t + q(t) \tag{16}$$

where $a\sin\omega t$ denotes the limit cycle oscillation and $q(t)$ represents the superimposed signals. As $q(t)$ will primarily be caused by the error signal $(\mathbf{x}_d - \mathbf{x})$, it can be assumed that it varies much more slowly than $\sin\omega t$ and that it is smaller in magnitude than a, assumptions which are certainly true near the steady state (when the oscillations occur) as the model and process outputs are similar. Since $q(t)$ varies slowly it can be approximated by a constant in the above equation [22], so that

$$w(t) \approx a\sin\omega t + q. \tag{17}$$

If such a signal existed within the system, the output from the nonlinearity would appear as in Fig. 3(b).

The output waveform $z(t)$ can be represented as a Fourier Series. In most real motoring control systems, the harmonics of the signal $z(t)$ will be greatly attenuated by $H(j\omega)$. $z(t)$ is therefore approximated by its fundamental component only.

The nonlinearity presents different transfer properties to the oscillation $a\sin\omega t$ and the "d.c. signal" q. The describing function with which the nonlinearity is modeled, when considering oscillations, is given by [21]

$$F(a) \approx \frac{K}{\pi}[\sin^{-1}\theta + \sin^{-1}T\theta + \theta(\cos(\sin^{-1}\theta) + T\cos(\sin^{-1}T\theta))] \tag{18}$$

where $K = \frac{K_1}{K_2}$, $T = (U + Kq)/(U - Kq)$ and $\theta = (U - Kq)/Ka$. It has been assumed that $F(a)$ is approximately real valued, since the phase shift caused by the d.c. offset is small.

$F(a)$ in (18) is used to describe the nonlinearity in further analysis. The system presented to the sustained oscillation consists of a closed loop containing $F(a)$ and the remaining linear elements from Fig. 2, which can be represented as a single linear transfer function $G(j\omega)$ given by

$$G(j\omega) = H(j\omega)\left[1 + \frac{M}{K_1}(j\omega)^2\right]. \tag{19}$$

The condition for sustained oscillations within the system is that the oscillation propagates around the system without distortion. This condition is met if the amplitude a and the frequency ω of the oscillation are such that $G(j\omega) = \frac{-1}{F(a)}$. The general result can therefore be noted, that the intersection of $G(j\omega)$ and $\frac{-1}{F(a)}$ on a Nyquist Diagram indicates an oscillation. Small perturbations in the amplitude a shows this oscillation to be stable for this describing function $F(a)$ [21]. The amplitude a will itself be a function of the frequency ω.

Determining the maximum value of $\frac{-1}{F(a)}$, which can be derived from (18), gives the region, within the Nyquist plane, in which $\frac{-1}{F(a)}$ exists. The function is at its maximum when $\theta = \frac{1}{T}$ and then has value

$$\frac{-1}{F(a)_{\max}} \approx -\frac{\pi}{K}\left[\sin^{-1}\left(\frac{U-Kq}{U+Kq}\right) + \frac{\pi}{2} + \left(\frac{U-Kq}{U+Kq}\right) \times \cos\left(\sin^{-1}\left(\frac{U-Kq}{U+Kq}\right)\right)\right]^{-1}. \tag{20}$$

The function exists for all values of a in the region $\frac{U+Kq}{K} < a < \infty$.

The effect of using this function will now be considered with different controllers for $N(s)$, and the particular vehicle dynamics $D(s)$ (see Fig. 2), along with their effect upon a possible intersection of the resulting $G(j\omega)$ and $-1/F(a)$ curves.

IV. Application to Real Vehicles

In this section, conditions upon K_1 and K_2 for two different mobile robots, with position control systems as in Fig. 2 are derived. The first of these (named Eric) weighs only 4.8 kg and was built using two permanent magnet d.c. motors [23], and is controlled by an *integral* speed controller. The second vehicle is tracked and was initially built for military purposes and weighs 62 kg. Again, it is driven by d.c. motors, but its speed controller is a *proportional* one.

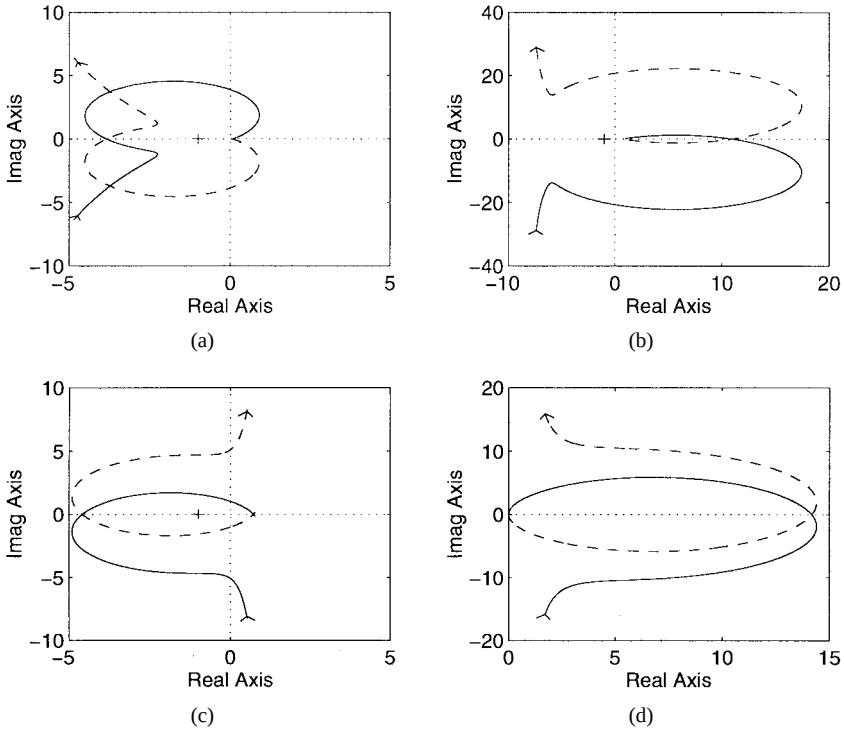

Fig. 4. Nyquist plots for $G(j\omega)$, when $N(s)$ is a P.I.D. controller, for various conditions on the time constants. (a) $T_8, T_9, T_{10} \gg T_6, T_7$, (b) T_8, T_9, T_{10} are slightly larger than T_6, T_7, (c) $T_8, T_9, T_{10} \approx T_6, T_7$, and (d) $T_8, T_9, T_{10} \ll T_6, T_7$. The arrow heads show the directions of increasing frequency.

A. Avoiding Limit Cycles With Various Combinations of P.I.D. Control

The prevention of limit cycle oscillation occurs if

$$\frac{-1}{F(a)_{\max}} > -|G(j\omega_0)| \tag{21}$$

for all values of q as $q \to 0$. This condition, under full P.I.D. control, is now examined. In a full P.I.D. system. $G(j\omega)$ would be of the form

$$G(j\omega) = \frac{Q(1+j\omega T_6)(1+j\omega T_7)\left(1-\frac{M}{K_1}\omega^2\right)}{j\omega(1+j\omega T_8)(1+j\omega T_9)(1+j\omega T_{10})} \tag{22}$$

where the time constants T_6 to T_{10} and Q are related to the motoring and control parameters in $N(s)$ and $D(s)$.

The frequency response of $G(j\omega)$ for various conditions upon the time constants T_6 to T_{10} in (22) can be observed in Fig. 4. It can be seen, without the use of further algebra, that P.I.D. Nyquist curves may have negative real axis crossing points, meaning that stable oscillations are possible.

If the time constants T_6 to T_{10} in this equation are of the same order of magnitude, then $G(j\omega)$ becomes an "all pass" transfer function meaning that, unless K_1 is large, $z(t)$ can no longer be approximated by its fundamental component only. Under these conditions the combination of full P.I.D. control and the proposed acceleration feedback system would require a more in depth analysis into higher order oscillations.

It will now be shown, that full P.I.D. control is unnecessary within the overall position servo loop. This is because the time optimal bang bang control $(K_1/K_2 \to \infty)$ is almost attainable without the possibility of oscillation with proportional or integral speed control alone[4]. To demonstrate this, goal seeking results are presented using various values for the attractive force constant K_1 and the dissipative force constant K_2. Eric's integral only, speed control system is considered first (see [12] for an analysis of motor parameter estimation techniques).

1) Goal Seeking Using Eric: Entering the numerical motoring parameters for Eric into inequality 21, gives the following condition for no oscillations, as $q \to 0$[5]

$$K_1 < 330K_2 + 2072. \tag{23}$$

In the first experiment, a position vector $\mathbf{x}_d$ was injected into the system of Fig. 2 at time $t = 0$. This vector required the mobile robot to rotate through approximately 24° during the initial part of its trajectory, in order to face the target at $\mathbf{x}_d$. The mobile was able to rotate at a maximum angular speed of 36.4°/s and values for K_1 and K_2 were initially chosen, which violate inequality 23. For a perfect system, the input voltage to the motor controller (V in Fig. 2) would be expected to vary with time as in the top left hand graph in Fig. 5. A 'perfect' response to this input would vary with time as in the bottom left hand curve.

The right hand curves show the actual response of the vehicle, for the chosen values of K_1 and K_2. When the mobile faces its target (after about 0.7 seconds), the chosen values of K_1 and K_2 cause oscillation. Note that the frequency is approximately 3.8 Hz which is close to that suggested by the describing function analysis. The lower right hand graph also

[4]It should of course be noted that although not theoretically necessary for time optimal convergence, integral action can be beneficial to a system's response in the presence of unmodeled effects such as stiction [24].

[5]Note that this inequality is the result of an approximate analysis and it can therefore be expected to only approximately predict K_1 and K_2 at oscillation.

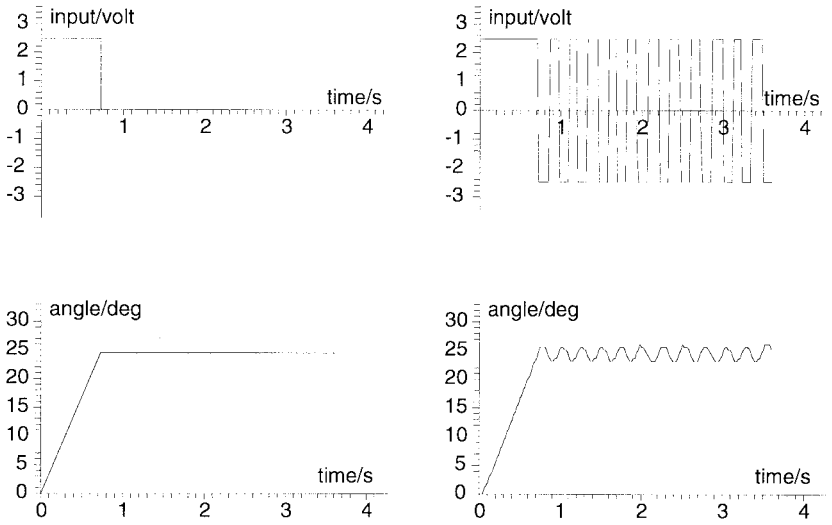

Fig. 5. Graphs showing the speed signals produced by the nonlinearity and the output angular position of the mobile when pursuing its target. The left-hand graphs show the results expected for a perfect system when using a high value for K_1/K_2, so that the nonlinearity approximates a perfect relay. The right-hand graphs show the actual response when $K_1 = 20\,000$ and $K_2 = 10$ thus providing a high gain which violates inequality 23.

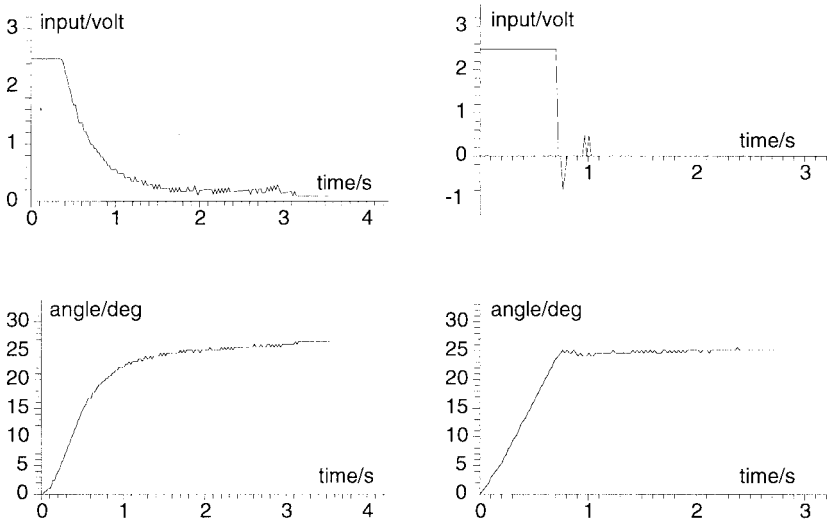

Fig. 6. Left-hand graphs show results using $K_1 = 2000$ and $K_2 = 40$ thus obeying the conditions for no oscillations. Note the slow response as the vehicle moves toward the correct angle. The right-hand graphs show the nonlinearity output and position when $K_1 = 20$ and $K_2 = 0.01$ thus obeying the above conditions for no oscillations. $K_1/K_2 = 2000$ thus allowing convergence to the correct angle in the same time as the oscillatory response in the first experiment of approximately 0.8 s. The same start and goal coordinates were used in each case.

shows that the amplitude of the input oscillation Ka (produced by the nonlinearity) is indeed much greater than the d.c. offset Kq since once the oscillatory mode begins, its average value does not appear to change. The initial assumption that $a \gg q$ in (18) seems to be justified.

The left hand graphs in Fig. 6 show the motor input speed signal and angular position versus time for the same initial and target positions of the robot when the individual values of K_1 and K_2 obey inequality 23. In addition, the slope of the linear section within the nonlinearity, K_1/K_2 is much lower than before. No oscillation results as the mobile asymptotically positions itself on target for its goal. It can also be seen from the graphs however that the time taken to reach the required angle is significantly increased because of the low gradient.

It is in response to this effect that the acceleration feedback term, derived from energy considerations, shows its advantage over position feedback only. Without this term, $|G(j\omega)|$ becomes independent of K_1 and under these conditions inequality 23 would become

$$K_1 < 330K_2 \tag{24}$$

using Eric's motor parameters. To measure the acceleration correctly, either inertial sensors or accelerometers should be used. In the experiments carried out here, the odometer outputs were simply numerically differentiated twice using a Lagrange five-point formula, to produce somewhat noisy but adequate acceleration estimates [25].

Equation (24) would impose an upper limit on the gradient of the speed controller K_1/K_2 of approximately 330. However, with the acceleration term, inequality 23 suggests that the value of K_1/K_2 can be increased beyond 330 without oscillation, meaning that maximum speed can be maintained during a higher percentage of a mobile robot's trajectory to its target.

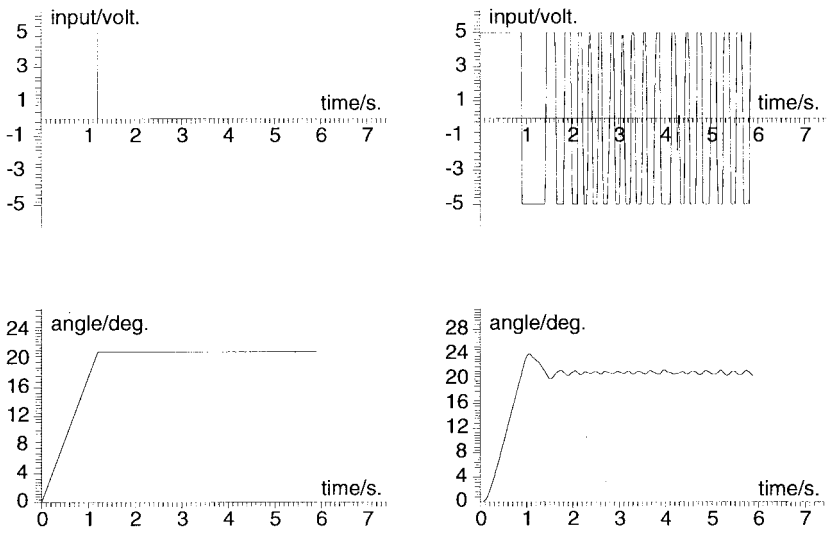

Fig. 7. Response of the tracked vehicle to target vector inputs. K_1 was set to 50 000 and K_2 was set to 1.0 in order to violate inequality 25 and observe oscillations.

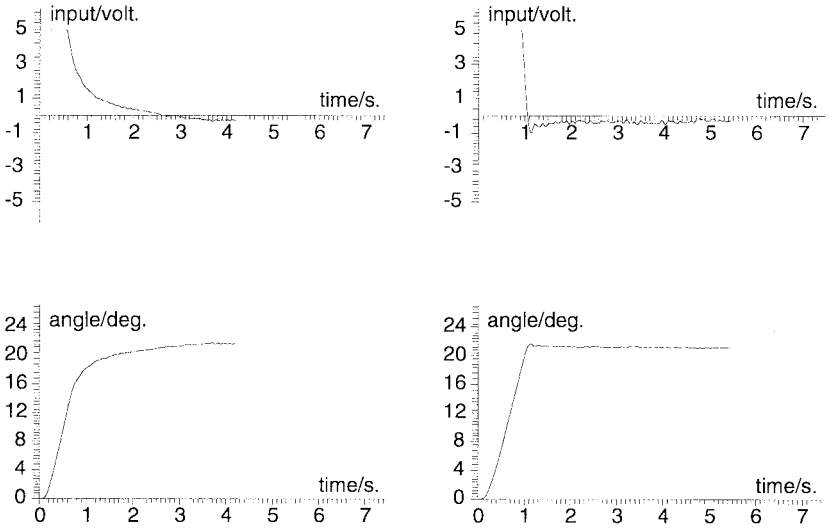

Fig. 8. Slow and fast asymptotically stable response of the tracked mobile robot. The left hand graphs show the result when $K_1 = 120$ and $K_2 = 1.0$. The vehicle asymptotically approaches its target but the response speed is slow. The right hand curves demonstrate the advantage offered by the acceleration feedback as the response speed is increased by selecting $K_1 = 350$ and $K_2 = 1.0$, satisfying inequality 25.

The right hand graphs in Fig. 6 show the results of the input voltage supplied by the nonlinearity to the motors and output angular position. The correct angular position is reached in the same time (approximately 0.8 seconds) as that shown in Fig. 5, but this time without oscillation.

2) Goal Seeking Using a Tracked Vehicle: Using the estimated motoring parameters for the proportional only, speed controlled, tracked vehicle (see [12]), the following condition for no oscillations results:

$$K_1 < 235K_2 + 32\,194. \tag{25}$$

Once again it can be seen that the acceleration feedback term provides a constant in the above inequality which allows us to increase the gradient K_1/K_2 well beyond 235, the maximum permissible value without acceleration feedback.

Figs. 7 and 8 show the results of similar experiments to those in Section IV-A1, this time using the tracked vehicle.

Note once again, that if individual values of K_1 and K_2 satisfy inequality 25, and K_1/K_2 is much larger than that allowed without acceleration feedback, stable asymptotic convergence results at a much higher rate.

V. Conclusions

A link has been established between the aspects of navigation, in the form of goal seeking and obstacle repulsion, and the control of a mobile vehicle.

Artificial potential fields provide a useful tool for deriving control laws which are naturally suited to any vehicle, since its total energy provides a single function which incorporates the local goal seeking parameters. The 'energy function' associated with a mobile robot under the influence of an imaginary potential field, can be used to assess the conditions

under which global asymptotic stability is guaranteed with respect to a desired position vector $\mathbf{x}_d$.

Any real vehicle will automatically inherit a nonlinear position control system, when tracking a target. Irrespective of particular motor dynamics or speed controllers, a simple potential attraction law between a target and mobile robot can result in limit cycle oscillations when in pursuit of the target.

The application of the nonlinear theory allows a time optimal control system to be designed. This is aided by the acceleration feedback term which is extremely effective, since it produces an extremely stable, yet high speed, response. Without inertial sensors or accelerometers, the problem of measuring acceleration in the presence of noisy encoder signals must be addressed, and a suitable numerical algorithm applied which gives fast, low noise acceleration estimates.

ACKNOWLEDGMENT

The author would like to thank P. J. Probert, SERC, for his support.

REFERENCES

[1] E. Freund and R. Mayr, "Nonlinear path control in automated vehicle guidance," *IEEE J. Robot. Automat.*, vol. 13, pp. 49–60, Feb. 1997.
[2] Z. Shiller and Y. R. Gwo, "Dynamic motion planning of autonomous vehicles," *IEEE J. Robot. Automat.*, vol. 7, pp. 241–249, Apr. 1997.
[3] B. Thuilot, B. d'Andrea Novel, and A. Micaelli, "Modeling and feedback control of mobile robots equiped with several steering wheels," *IEEE J. Robot. Automat.*, vol. 12, pp. 375–390, June 1996.
[4] S. Wane and A. Schmitt, "Dynamic control of the execution of trajectories by a mobile robot," in *Proc. Int. Conf. Intell. Robots Syst.*, 1991, pp. 199–204.
[5] D. E. Koditschek, *Robot Planning and Control Via Potential Functions—From the Robotics Review*. Cambridge, MA: MIT Press, 1989.
[6] Y. K. Hwang and N. Ahuja, "A potential field approach to path planning," *IEEE J. Robot. Automat.*, vol. 8, pp. 23–32, Feb. 1992.
[7] ——, "Path planning using a potential field representation," Tech. Rep. UILU-ENG-88-2251, Univ. of Illinois at Urbana-Champaign, 1988.
[8] O. Khatib, "Real-time obstacle avoidance for manipulators and mobile robots," in *Proc. IEEE Int. Conf. Robot. Automat.*, St. Louis, Mar. 1985, pp. 500–505.
[9] E. Rimon and D. E. Koditschek, "Exact robot navigation by means of potential functions: Some topological considerations," in *Proc. IEEE Int. Conf. Robot. Automat.*, 1987, pp. 1–6.
[10] J.-C. Latombe, *Robot Motion Planning*. Norwell, MA: Kluwer, 1991.
[11] R. Weinstock, *Calculus of Variations*. New York: Dover, 1974.
[12] M. D. Adams, "Optical range data analysis for stable target pursuit in mobile robotics," Ph.D. thesis, Univ. of Oxford, Oxford, U.K., 1992.
[13] P. Khosla and R. Volpe, "Superquadric artificial potentials for obstacle avoidance and approach," in *IEEE J. Robot. Automat.*, pp. 1778–1784, 1988.
[14] M. D. Adams and P. J. Probert, "Mobile robot motion planning—Stability, convergence and control," in *Int. Conf. Intell. Robots Syst.*, 1991, pp. 1019–1024.
[15] K. Kosuge, H. Takeuchi, and K. Furuta, "Motion control of a robot arm using joint torque sensors," *IEEE J. Robot. Automat.*, vol. 6, pp. 258–262, Apr. 1990.
[16] M. S. Branicky, "Multiple Lyapunov functions and other analysis tools for switched and hybrid systems," *IEEE Trans. Automat. Contr.*, vol. 43, pp. 475–482, Apr. 1998.
[17] C. W. Warren, "Global path planning using artificial potential fields," in *IEEE J. Robot. Automat.*, p. 316, 1989.
[18] G. M. T. D'Eleuterio and C. J. Damaren, "The relationship between recursive multibody dynamics and discrete time optimal control," *IEEE J. Robot. Automat.* , vol. 7, pp. 743–749, Dec. 1991.
[19] J. Guckenheimer and P. Holmes, "Nonlinear oscillations, dynamical systems and bifurcations of vector fields," *Appl. Math. Sci.*, vol. 42, 1990.
[20] R. Murray-Smith and T. A. Johansen, Eds., *Multiple Model Approaches to Modeling and Control*. Bosingstoke, U.K.: Taylor and Francis, 1995.
[21] O. L. R. Jacobs, *Introduction to Control Theory*. Oxford, U.K.: Clarendon Press, 1974.
[22] K. J. Astrom and B. Wittenmark, *Adaptive Control*. Reading, MA: Addison Wesley, 1988.
[23] M. D. Adams, "A mobile robot platform," Tech. Rep., Robot. Res. Group, Oxford Univ., Oxford, U.K., 1988.
[24] P. Levi, "Principles of planning and control concepts for autonomous mobile robots," in *IEEE J. Robot. Automat.*, pp. 874–882, 1987.
[25] E. Kreysig, *Advanced Engineering Mathematics*, 5th ed. New York: Wiley, 1983.

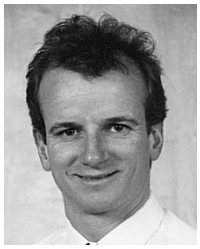

Martin D. Adams (S'90–A'96) received the degree in engineering science and the D.Phil. degree both from the University of Oxford, U.K., in 1988 and 1992, respectively.

He then moved to Switzerland, where he continued his research as a Post-doctoral Research Assistant at the Institute of Robotics, Swiss Federal Institute of Technology, Zurich, Switzerland. He was employed as a Guest Professor and taught control theory in Buchs, St. Gallen, Switzerland, from 1994 to 1995. Since September 1996, he has been a Research Scientist in Robotics and Control at the European Semiconductor Equipment Centre (ESEC), Cham, Switzerland. His interests include adaptive control, mobile robot navigation, sensor design, and data interpretation.